SCIENCE CHINA
Earth Sciences

• RESEARCH PAPER •

September 2012 Vol.55 No.9: 1480–1488
doi: 10.1007/s11430-012-4406-3

End-Guadalupian mass extinction and negative carbon isotope excursion at Xiaojiaba, Guangyuan, Sichuan

WEI HengYe[1,2*], CHEN DaiZhao[1], YU Hao[1,2] & WANG JianGuo[1]

[1]*Key Laboratory of Petroleum Resources Research, Institute of Geology and Geophysics, Chinese Academy of Science, Beijing 100029, China;*
[2]*Graduate University of Chinese Academy of Sciences, Beijing 100049, China*

Received April 21, 2011; accepted October 20, 2011; published online April 12, 2012

The end-Paleozoic biotic crisis is characterized by two-phase mass extinctions; the first strike, resulting in a large decline of sessile benthos in shallow marine environments, occurred at the end-Guadalupian time. In order to explore the mechanism of organisms' demise, detailed analyses of depositional facies, fossil record, and carbonate carbon isotopic variations were carried out on a Maokou-Wujiaping boundary succession in northwestern Sichuan, SW China. Our data reveal a negative carbon isotopic excursion across the boundary; the gradual excursion with relatively low amplitude (2.15‰) favors a long-term influx of isotopically light ^{12}C sourced by the Emeishan basalt trap, rather than by rapid releasing of gas hydrate. The temporal coincidence of the beginning of accelerated negative carbon isotopic excursion with onsets of sea-level fall and massive biotic demise suggests a cause-effect link between them. Intensive volcanic activity of the Emeishan trap and sea-level fall could have resulted in detrimental environmental stresses and habitat loss for organisms, particularly for those benthic dwellers, leading to their subsequent massive extinction.

mass extinction, Emeishan trap, sea-level fall, carbon cycle, end-Guadalupian, Guangyuan, SW China

Citation: Wei H Y, Chen D Z, Yu H, et al. End-Guadalupian mass extinction and negative carbon isotope excursion at Xiaojiaba, Guangyuan, Sichuan. Sci China Earth Sci, 2012, 55: 1480–1488, doi: 10.1007/s11430-012-4406-3

The end-Guadalupian (end-Middle Permian) biotic crisis was considered the first strike of the end-Permian mass extinction, in the Phanerozoic times [1–3]. During this crisis, marine biota suffered a decline rate of 50% at generic level; although lower than that at the end-Permian (67%), it is higher than that at the end-Frasnian (41%), end-Triassic (46%), and end-Cretaceous (45%) mass extinctions [4]. This crisis is characterized by the massive losses of keriothecal-walled fusulinaceans [4, 5] and corals [5, 6], and turnover in calcareous algae [4, 5]. Some invertebrate taxa such as brachiopods [7–9] and ammonoids [3, 10–13] suffered relatively minor losses while bryozoans [9], bivalves [14–17] and gastropods [18] experienced a minor decrease in diversity [19]. Since the International Commission of Stratigraphy ratified the Penglaitan section at Laibin, Guangxi, South China as the Guadalupian-Lopingian Stage boundary of Global Stratotype Section and Point (GSSP), which was placed slightly below the top of Maokou Formation in 2005 [20], increasing interests arise in the end-Guadalupian biota crisis in South China [11, 21–24]. Recent studies suggest that the extinction horizon of marine microfossil occurs in the middle of the Capitanian Stage [11, 21–24], below the Guadalupian-Lopingian (G-L) boundary. However, causes of this biotic crisis remain highly debatable. Most of the researchers suggested that the end-Guadalupian crisis was triggered by the eruption of Emeishan large igneous province (LIP) [3, 21, 25] in South China and the dwelling-space loss of marine habitants caused by marine regression at the end of Capitanian age [1, 8, 26, 27]. In this

*Corresponding author (email: weihengye@yahoo.com.cn)

paper, detailed sedimentology, fossil record and carbon isotope analyses were carried out upon the newly discovered Maokou-Wujiaping boundary section at Chaotian, Guangyuan City, northern Sichuan, South China, to provide additional lines of evidence for the mass extinction.

1 Geological setting

1.1 Location of the study section

The study section is located in a valley (32°38.25′N, 105°53.35′E), about 300 m away from the Xiaojiaba bridge of No. 108 national highway to the east of Chaotian town, Guangyuan, northern Sichuan, South China (Figure 1(a)). Previous studied sections of Permian at Chaotian area are located in a narrow gorge called Mingyuexia to the South of Chaotian town [27–30] (Figure 1(a)), ~5 km away from the Xiaojiaba section in this paper.

1.2 Stratigraphy and sedimentology

During the Permian, Chaotian area was located in the northwestern margin of Yangtze Platform [31], where the carbonate (ramp) platform evolved into a basinal environment during the Late Permian. The strata deposited include, in ascending order, the Chihsia and Maokou formations of Middle Permian, and Wujiaping, Dalong and Changhsing formations of Upper Permian. Except the Dalong Formation composed of basinal bedded chert interbedded with black shales, they mostly consist of limestone. According to Jin et al.'s subdivisions of the Permian System in China [32], the Maokou Formation includes the lower Roadian, Wordian and Capitanian stages of Middle Permian. The conodont biozones in the Capitanian, in the ascending order, consist of *J. postserrata*, *J. shannoni*, *J. altudaensis*, *J. prexuanhanensis*, *J. xuanhanensis*, *J. granti*, and *C. postbitteri hongshuensis* [24].

Tectonically, the Xiaojiaba section is located on the northern limb of Mingyuexia anticline. At this locality, the Maokou (Guadalupian), Wujiaping (Wujiapingian), Dalong, Changhsing, and Feixianguan formations (Lower Triassic) successively crop out along the roadcut (Figure 1(b)). The Maokou-Wujiaping boundary succession crops out fairly completely (Figure 1(c)). We measured and sampled the upper part of Maokou Formation and the lower part of the Wujiaping Formation (17.5 m in thickness).

The measured interval of Maokou Formation displays metre-scale shallowing-upward cycles comprising basal

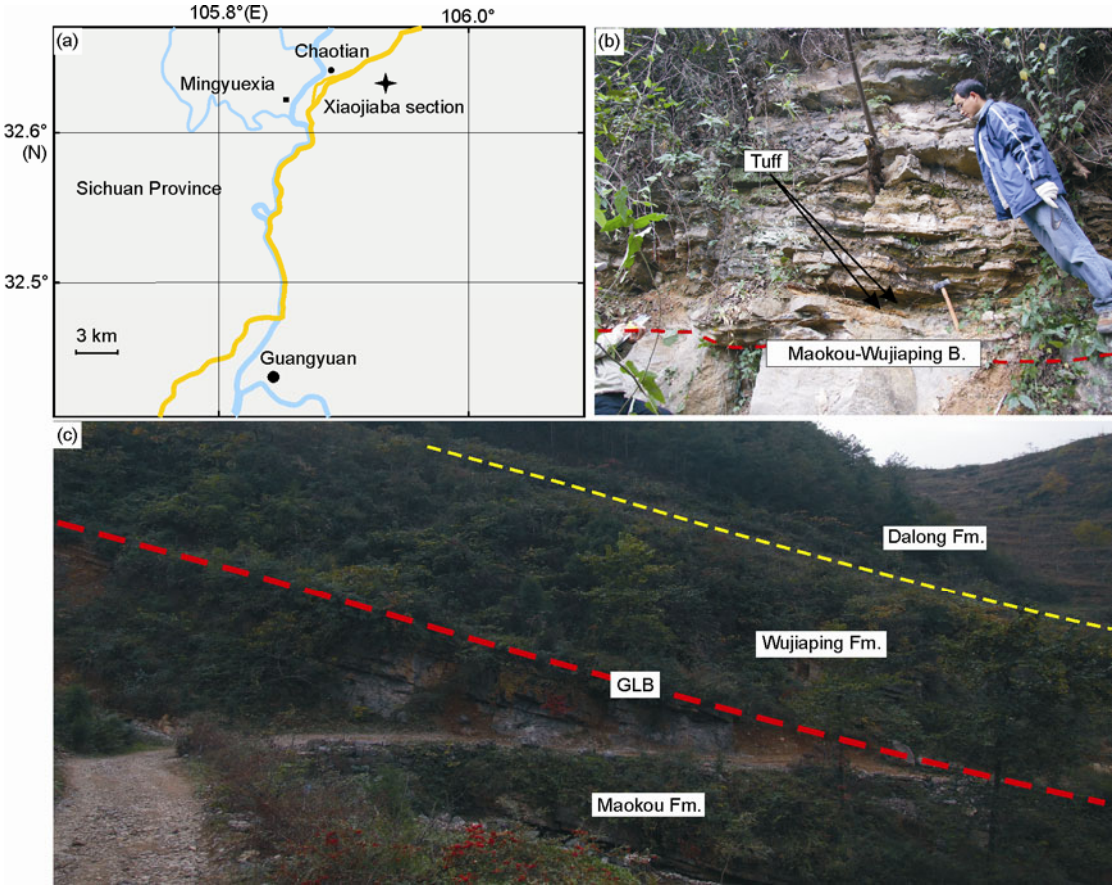

Figure 1 The Xiaojiaba section in northern Guangyuan, Sichuan, China. (a) Location of the Xiaojiaba section; (b) outcrop of the Maokou-Wujiaping boundary succession; (c) panoramic view of Xiaojiaba section.

thick-bedded grey bioclastic packstones bearing abundant chert bands, which pass upward into massive bioclastic packstones commonly with chert nodules (Figure 2). In contrast, the uppermost cycles in Maokou Formation is absent of chert nodules/bands (Figures 1(c) and 2). Two thin layers of brownish tuffaceous claystones are intercalated, at thickness of 2.1 and 5.7 m, respectively, in measured interval (Figure 2); the brownish coloration likely resulted

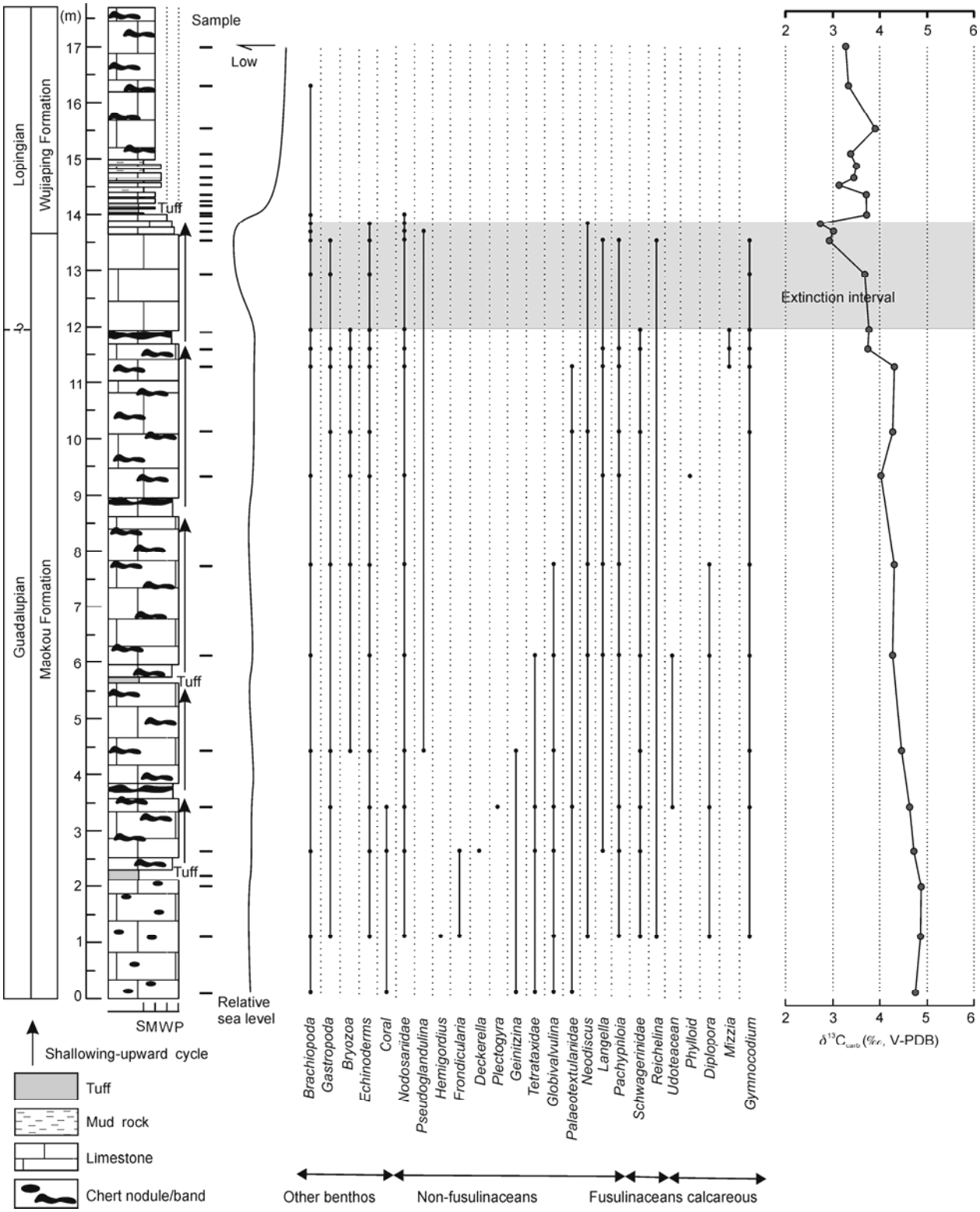

Figure 2 Sedimentary succession, occurrences of foraminifers and calcareous algae, and carbonate carbon isotopic variations across the Maokou-Wujiaping boundary at Xiaojiaba, northern Sichuan. S, shale; M, lime mudstone; W, wackestone; P, packstone.

from subaerial weathering [28]. The overlying Wujiaping Formation starts with three beds of thin-bedded lenticular argillaceous bioclastic wackstones to packstones, followed by siliceous shales and limestones intercalated (or interbedded) with tuffaceous beds (two beds) and shales (Figures 1(c) and 2), in which radiolarians were found. Euhedral ziron crystals were extracted from the tuffaceous layers. Further upwards, rocks mainly comprise medium- to thick-bedded lime mudstones bearing chert nodules/bands (Figure 2). It is worthwhile to note an apparent change in lithofacies across the Maokou-Wujiaping boundary, i.e., apparent increase in argillaceous matter and decrease in bed thickness. Bioturbations occur in the thin-bedded lenticular limestones at the base of the Wujiaping Formation. No subaerial exposure and submarine erosions were identified in the rocks in the boundary successions.

2 Methods

Thirty fresh samples were taken from studied interval with sampling spacing of ~0.17 m just across the boundary but slightly sparse (0.88 m) away from the boundary. Twenty-seven petrographic thin sections were prepared for facies analysis and fossil identification. After detailed petrographic examination, powders were obtained from the micrite matrix using the micro-drill, avoiding diagenetic admixture. ~5 mg powders for carbon and oxygen isotopic analysis were reacted with 100% phosphoric acid at 50°C for 24 h. Isotopic ratios were measured on a Finnigan MAT-251 mass-spectrometer using the CO_2. The reference material (GBW04405, Zhoukoudian limestone in China) was used to calibrate the mass spectrometer. Reproducibility based on the standards is better than 0.2‰. Carbon and oxygen isotope ratios are expressed as δ-notation in per mille (‰) relative to V-PDB standard. Analytical precision for both δ^{13}C and δ^{18}O is better than 0.014‰ (1σ). The isotope ratios were measured at the Stable Isotope Laboratory in the Institute of Geology and Geophysics, Chinese Academy of Sciences.

3 Results

3.1 Depositional environments and biotic successions

The Maokou Formation at Xiaojiaba section consists mainly of bioclastic packstones containing abundant benthic fossils such as foraminifer, fusulinacean, calcareous algae, coral, brachiopod, gastropod, bryozoan and echinoderm. The biotic assemblage and presence of chert nodules/bands in the rock indicates a slightly deep carbonate platform environment (i.e., open marine moderate to deep subtidal). By contrast, the absence of chert nodules/bands in the uppermost massive limestones of Maokou Formation suggests a shallower water condition; the thickness-decreasing depositional cycle is likely a reflection of platform shallowing as well. However, the absence of subaerial exposure indicators on the top of Maokou Formation suggests that carbonate platform was not subject to emergence above sea level. The apparent decrease in bed thickness and the occurrence of bioturbation, but increase in argillaceous matter in the basal carbonates of Wujiaping Formation, indicate a significant drop in carbonate production rate per time, implying a rapid deepening during deposition. The presence of radiolarians, although with minor amounts, in the lowermost Wujiaping Formation also suggests deepening of deposition. Compared with the deepest facies (basinal facies) of black bedded cherts and shales in the overlying Dalong Formation, the carbonate rocks, especially in the basal Wujiaping Formation, were likely deposited in deep subtidal condition with little storm agitation. The transition from progradational to retrogradational patterns across the Maokou-Wujiaping boundary, which can also be seen extensively across the G-L boundary at the Penglaitan section (GSSP section) and elsewhere [22], likely represents the transition from sea-level fall at the end-Guadalupian [22] and subsequent sea-level rise in the beginning of Lopingian [24].

The fusulinacean foraminifers in the Maokou Formation at Xiajiaba section include *Schwagerinidae* and *Reichelina*. The *Reichelina* is a survivor genus across the G-L boundary, so is common in both the upper Capitanian and lower Wujiapingian [22]. The keriothecal-walled *Schwagerinidae* is one of the extinction families; it disappears at the thickness of 12 m near the top of Maokou Formation where obvious facies changes take place as well, defining the extinction horizon (Figure 2) [24]. The non-fusulinacean foraminifers consist mainly of small foraminifers, including *Nodosariidae*, *Pseudoglandulina*, *Hemigordius*, *Frondicularia*, *Deckerella*, *Plectogyra*, *Geinitzina*, *Tetrataxidae*, *Globivalvulina*, *Palaeotextulariidae*, *Neodiscus*, *Langella*, and *Pachyphloia* (Figure 2), in which the *Nodosariidae* is the most common. At this locality, the calcareous algae include *Udoteacean*, *Phylloid*, *Diplopora*, *Mizzia*, and *Gymnocodium* (Figure 2), in which *Udoteacean* and *Mizzia* were extinct in this crisis while *Gymnocodium* survived the crisis. The calcareous alga *Mizzia* disappeared just at the extinction level, indicating the beginning of turnover of calcareous algae.

3.2 Carbon isotopes

At the study section, the carbonate δ^{13}C values range from 2.74‰ to 4.89‰ (VPDB) and δ^{18}O values range from −7.15‰ to −2.88‰ (VPDB) (Table 1). Based on the cross-plot of $\delta^{13}C_{carb}$ and δ^{18}O (Figure 3), no covariance is visible between them (R^2=0.020), suggesting no significant alteration of carbon isotope composition during diagenesis. The δ^{13}C values are relatively high from the base to the thickness of 2 m (4.89‰), in which a small negative shift of 0.57‰ magnitude can be recognized from the thickness of 2 m (i.e., the first tuff layer) to 10 m. Upwards, an accelerated

Table 1 Analytical results of stable carbon and oxygen isotopic ratios of carbonates at Xiaojiaba section, Guangyuan, South China

Sample No.	Thickness (m)	$\delta^{13}C$ (‰)	$\delta^{18}O$ (‰)
Maokou Formation			
CT01	0.10	4.77	–6.06
CT02	1.10	4.88	–6.12
CT03	2.00	4.89	–6.14
CT05	2.63	4.74	–5.73
CT06	3.43	4.65	–5.72
CT07	4.43	4.47	–5.20
CT08	6.13	4.27	–5.62
CT09	7.73	4.31	–4.73
CT10	9.33	4.03	–5.88
CT11	10.13	4.27	–5.26
CT12	11.28	4.32	–4.14
CT13	11.58	3.76	–5.57
CT14	11.93	3.78	–5.67
CT15	12.93	3.68	–5.28
CT16	13.53	2.93	–6.16
CT17	13.68	3.02	–5.57
CT18	13.83	2.74	–5.60
CT19	13.98	3.72	–7.15
Wujiaping Formation			
CT23	14.35	3.71	–3.10
CT24	14.52	3.14	–3.23
CT25	14.65	3.47	–4.44
CT26	14.86	3.52	–3.16
CT27	15.08	3.39	–6.72
CT28	15.53	3.92	–2.88
CT29	16.28	3.34	–6.02
CT30	16.98	3.30	–5.28

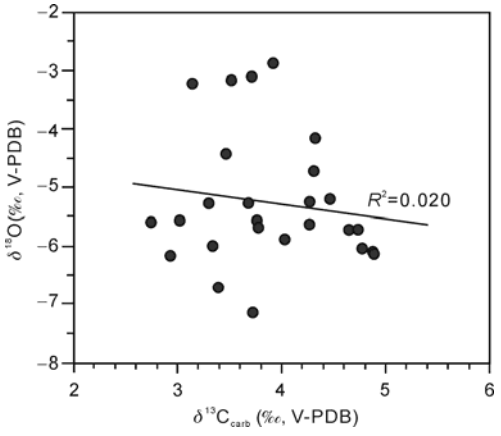

Figure 3 Cross-plot of $\delta^{13}C_{carb}$ and $\delta^{18}O$ values. No covariance is recognized between them.

negative excursion starts near the top of Maokou Formation (at 11.5 m), and reaches the trough (2.74‰), with an overall magnitude of 2.15‰, in the lenticular limestones of the lowermost Wujiaping Formation, above which $\delta^{13}C$ values rapidly return, although fluctuating, to higher values between 3‰ and 4‰. It is also noted that the onset of this major negative $\delta^{13}C$ excursion approximately coincides with the commencements of sea-levels fall and massive biotic demise.

4 Discussion

4.1 Emeishan large igneous province

From the Middle Permian, the huge basalt suite, well known as the Emeishan Basalt, was formed extensively on the southwest flank of Yangtze Platform. It covered an area of ca. 2.5×10^5 km^2, with a volume of ~0.3×10^6 km^3 [33], representing a large igneous province (LIP). This LIP consists mainly of flood basalts, contemporaneous mafic and felsic intrusions, and a small quantity of volcaniclastic rocks and tuffites [34, 35]. Some researchers suggested that the Emeishan LIP was formed in relation to mantle plume activity [36, 37]. However, the area of crustal uplift prior to volcanic eruption is relatively small, only about 1/20 to 1/25 times [37] of that predicted by the thermal plume model of Griffiths and Campbell [38]. The uplift was restricted to a small area [39], not as the large-scale doming as previously suggested [39–41]. The Emeishan LIP started massive eruption in the middle Capitanian age [21, 22, 42–44], spanning a period of $\leqslant$1 Ma [21, 45].

Although basalts occurred mainly within the inner zone around the eruptive center, tuffites (commonly as altered white claystones) were widespread on the Yangtze Platform, especially in the outer zone far away from the eruptive center. At Penglaitan, Guangxi, where the G-L boundary GSSP section is located, pyroclastic debris occur in the uppermost Maokou Formation and pale cream tuffaceous beds in the base of Heshan (or Wujiaping) Formation [20, 22]. At Xiaojiaba, tuffaceous beds occur in the upper part of Maokou Formation and in the base of Wujiaping Formation as well. At Mingyuexia section, ~5 km away from this study, the tuffaceous beds show a close geochemical affinity to the Emeishan volcanic rocks [29, 30]. These indicate the volcanic influences, although far-reaching, could have arrived at these areas in the outer zone of volcanic center. The synchronous sea-level fall at the end of Maokouian (or Guadalupian) time was probably contributed, to some extent, by the crustal doming in the course of LIP's eruptive activity. Although the age of these ash fallouts was not well constrained, He et al. [29, 30] reported a SHRIMP zircon U-Pb age of 260±5 Ma for the tuff (the Wangpo bed) across the Maokou-Wujiaping boundary at Mingyuexia not far from the study section, which can be temporally linked to the Emeishan basalt trap.

4.2 Negative carbon isotopic excursion

As stated above, the $\delta^{13}C$ values show a negative excursion near the top of Maokou Formation (at 11.5 m) and reach the

minimum (2.75‰) in the lowermost Wujiaping Formation, with an overall magnitude of 2.15‰, at studied section, and then quickly swing back, although slightly fluctuating. Similarly, a negative δ^{13}C shift was reported across the Maokou-Wujiaping boundary at Mingyuexia nearby, but with a larger magnitude of 8‰ [27]. By comparison, a coal seam occurs in the basal Wujiaping Formation at Mingyuexia section [27]; instead, thin-bedded siliceous shales and cherty limestone occur in the equivalent horizon at Xiaojiaba section, suggesting a deeper depositional setting there. Wang et al. [46] suggested that the magnitude of negative carbon isotopic excursion in shallow-water condition could be larger due to dissemination of nearshore light organic carbon matter [27, 47, 48]. It is worth noting that, at Penglaitan G-L boundary GSSP section in Guangxi, the major negative δ^{13}C excursion occurs near the top of Maokou to the basal Heshan (equivalent to Wujiaping) formations [46, 49]; similarly at Xiongjiachang section in Guizhou Province, it occurs in the transitional succession from Maokou to Wujiaping formations as well [21]. Although this negative excursion is found all within the Maokou-Wujiaping physical boundary successions, conodont zonation suggests different timing of this event at different localities. The reasons for this paradox may result from: 1) differences in depositional and/or ecological settings; 2) stratigraphic hiatus and/or erosion. Among these sections, the Penglaitan G-L GSSP boundary succession in Guangxi was deposited in the deepest setting, so that the conodont zones are most complete [49]. However, at Xiongjiachang section in Guizhou Province, it seems that the *J. granti* and *C. postbitteri hongshuensis* conodont zones are absent or missing [24], and at Mingyuexia, Sichuan Province, the *J. altudaensis* to *C. postbitteri hongshuensis* conodont zones are absent or missing [27]. To solve the inconsistencies between biostratigraphic, and lithostratigraphic and chemostratigraphic data, it is necessary to carry out further integrated studies.

The gradual negative δ^{13}C excursion with a relatively low magnitude (2.15‰) in parallel with the sea-level fall, and co-occurrence of concentrated tuffaceous layers (Figure 2) impling a volcanic driving from the far-reaching Emeishan basalt trap for this anomalous carbon cycling. The eruption of large LIP could release huge amounts of ^{12}C-rich CO_2 into atmosphere (δ^{13}C = −5‰) [50], leading to a negative carbon isotopic excursion of oceanic carbon pool through oceanic-atmospheric carbon transformation (or cycling) as if the LIP was large enough [51]. Dissociation of methane hydrates (δ^{13}C = −60‰ [52–54]) could have induced a rapid, larger-scale δ^{13}C excursion [55, 56]. Compared to the rapid excursion (faster than 1.5‰/kyr) of methane hydrate releasing, declining of the δ^{13}C values at Xiaojiaba is relatively mild. Given an estimate of 10 cm/ky for the carbonate accumulation rate [57], the negative carbon isotopic excursion of 0.74‰ from the thickness of 2 m to 11.5 m only produces a rate of 0.01‰/kyr of negative shift. Even the relatively rapid negative carbon isotopic excursion (1.58‰) from 11.5 m to 14 m just across the Maokou-Wujiaping boundary can only produce a rate of 0.06‰/ky of negative shift. Such a slow δ^{13}C excursion rate argues against methane releasing as the ^{12}C-enriched carbon source. Bond et al. drew a similar conclusion based on carbon isotopic variation patterns across the G-L boundary successions in southwestern China [24]. According to the model of Shelf et al. [58], eruption of 1000 km^3 magmas from the LIP can simultaneously result in CO_2 emission of about 13 Gt, such that, during the volcanic activity of Emeishan LIP, 1.3 times the amounts of modern atmosphere CO_2 (~3000 Gt) could have been simultaneously emitted into the atmosphere. In addition to the Emeishan basalt trap, end-Guadalupian plume-related alkaline intrusive suites [59] are documented in Oslo (Norway) [60, 61], Oman [62] and western Australia [63, 64] in the east of Pangea supercontinent. Therefore, the amounts of CO_2 emission during end-Guadalupian intensive volcanism could have largely exceeded the amounts previously estimated, resulting in the negative carbon isotopic excursion across the G-L boundary. However, it remains uncertain whether the end-Guadalupian abnormal carbon cycling was a single event, or multiple events.

4.3 Controls on the mass extinction

The end-Guadalupian biotic crisis is characterized by stepwise biotic decline [11]. Rugose corals and brachiopods first suffered from severe demise in the late Capitanian, then giant fusulinids stepped down in the end of Capitanian, and finally conodonts were turned over just prior to the G-L transition [11]. At Xiaojiaba, corals and non-fusulinacean foraminifers disappeared earlier, and extinction interval marked by the loss of fusulinacean *Schwagerinidae* occurred approximately in parallel with the major negative carbon isotopic excursion (Figure 2). As documented above, the negative shift is rationalized to be linked to the volcanism associated with the Emeishan LIP, thereby reasonably linking the mass extinction to the volcanism of Emeishan LIP at the end of Guadalupian as well. Based on Wignall et al.'s [22] observations, volcaniclastic deposits comprise one third of the total volcanic piles of Emeishan LIP, indicating more violent eruption than previously imaged. Generally, magmatic eruptions of LIP could release significant amounts of tephra and gases (CO_2, SO_2, HCl, HF and H_2O), of which SO_2 and CO_2 predominate. The Emeishan LIP was located in the tropical low-pressure zone [65] at the end of Guadalupian, favoring gas ascending. Moreover, the Emeishan LIP was geographically located in the eastern region of Pangea where trade wind prevailed, facilitating westward diffusion of tephra and gases. Therefore, the tephra and gases emitted probably could have been lofted to the mid- to upper-troposphere, and even to the base of stratosphere. In this case, the tephra and gases would spread

rapidly to other areas over the world, producing widespread tuff deposits across the G-L boundary in the Far East of Russia, South China, and Japan [59]. On the other hand, the SO_2 emitted would react with water vapors to form H_2SO_4 aerosols, as observed during the eruption of Laki volcano (1783) in Greenland, through which the aerosols spread over more widely than tephra did [66]. Because the diameter of aerosol particles is similar to the wavelength of visible light, the sulfate aerosols can scatter back and absorb the sun's radiation, resulting in short-lived cooling, thereby threatening the benthos adapting to tropical warm climate [67–70]. The fall of volcanogenic acid rains (H_2SO_4 and HCl) and the large flux of volcanogenic CO_2 and SO_2 into oceanic surface waters could have increased the water acidity and enhanced carbonate dissolution, thus preventing calcification of skeleton-secreting benthos in shallow waters [71].

As mentioned above, at Xiaojiaba, the extinction interval occurred in parallel with the sea-level drop, implying a causal link between them, at least a temporal coincidence, at the end-Guadalupian. Many studies proposed the lowest sea-level stand of the Paleozoic occurred at the end-Guadalupian [26], and only persisted for a short interval $\leqslant$2 Ma [72]. Firstly, decrease in ocean ridge volume may drive the sea-level fall as a result of diminished oceanic ridge accretion in the context of culmination of the Pangea supercontinent assembly at the end of Middle Permian. Secondly, regional doming caused by the impingement of superplumes below the base of the lithosphere could also result in the sea-level drop [26], which is rationalized by occurrences of several Middle-Late Permian LIPs in eastern Pangea [59]. By comparison, the latter case is more likely in view of the time interval of sea-level lowstand. During the Middle Permian, most islands and continental shelves favorable for benthic dwellers were located along the Paleo-Tethys and New-Tethys [8, 73], such that a rapid sea-level fall, likely caused by doming of LIPs, could have decreased the colonizing spaces of shallow-water benthic habitats and caused detrimental stresses on the organisms, together with volcanic-induced environmental deterioration, leading to their massive demise.

5 Conclusions

A negative carbon isotopic excursion with an overall magnitude of 2.15‰ took place just across the Maokou-Wujiaping boundary at Xiaojiaba, northern Sichuan. It was likely induced by the volcanic activity of the Emeishan LIP. This carbon isotopic anomaly co-occurred with the sea-level fall and massive biotic demise. Substantial loss of colonizing spaces of benthos and volcanic-induced environmental deterioration are likely the main factors responsible for the mass extinction at the end of Maokouian (or Guadalupian).

We thank Qiu Zhen, Zhou Xiqiang and Xiang Lei for their assistance in field work. Zhang Fusong is thanked for assistance in isotope analysis. This work was supported by National Natural Science Foundation of China (Grant No. 40839907).

1 Jin Y G, Zhang J, Shang Q H. Two phases of the end-Permian mass extinction. In: Embry A F, Beauchamp B, Class D J, eds. Pangea: Global Environments and Resources. Calgary: Canadian Society of Petroleum Geologists, Memoir 17, 1994. 813–822
2 Stanley S M, Yang X. A double mass extinction at the end of the Paleozoic era. Science, 1994, 266: 1340–1344
3 Wang X D, Sugiyama T. Diversity and extinction patterns of Permian coral faunas of China. Lethaia, 2000, 33: 285–294
4 Sepkoski Jr J J. Extinction and the fossil record. Geotimes, 1994, 39: 15–17
5 Wang X D, Sugiyama T. Diversity and extinction patterns of Permian coral faunas of China. Lethaia, 2000, 33: 285–294
6 Wang X D, Wang X J, Zhang F, et al. Diversity patterns of the Carboniferous and Permian rugose corals in South China. Geol J, 2006, 41: 329–343
7 Shen S Z, Shi G R. Diversity and extinction patterns of Permian Brachiopoda of South China. Histor Biol, 1996, 12: 93–110
8 Shen S Z, Shi G R. Paleobiogeographical extinction patterns of Permian brachiopods in the Asian-western Pacific Region. Paleobiology, 2002, 28: 449–463
9 Shen S Z, Zhang H, Li W Z, et al. Brachiopod diversity pattern from Carboniferous to Triassic in South China. Geol J, 2006, 41: 345–361
10 Jin Y G, Zhang J, Shang Q H. Pre-Lopingian catastrophic event of marine faunas. Acta Palaeontol Sin, 1995, 34: 410–427
11 Shen S, Shi G R. Latest Guadalupian brachiopods from the Guadalupian/Lopingian boundary GSSP section at Penglaitan in Laibin, Guangxi, South China and implications for the timing of the pre-Lopingian crisis. Palaeoworld, 2009, 18: 152–161
12 Zhou Z R. Early Permian ammonite-fauna from southeastern Hunan. In: Nanjing Institute of Geology & Palaeontology, Chinese Academy of Sciences, ed. Collective Papers of Graduate Students in Nanjing Institute of Geology & Palaeontology, Chinese Academy of Sciences (in Chinese). Nanjing: Science and Technology of Jiangsu Province Press, 1987. 285–348
13 Shen S Z, Shi G R. Latest Guadalupian brachiopods from the Guadalupian/Lopingian boundary GSSP section at Penglaitan in Laibin, Guangxi, South China and implications for the timing of the pre-Lopingian crisis. Palaeoworld, 2009, 18: 152–161
14 Powers C M, Bottjer D J. The effects of mid-Phanerozoic environmental stress on bryozoan diversity, paleoecology, and paleogeography. Glob Planet Change, 2009, 65: 146–154
15 Fang Z J. Approach to the Extinction Pattern of Permian Bivalvia of South China. In: Rong J Y, Fang Z J, eds. Mass Extinction and Recovery: Evidences from the Palaeozoic and Triassic of South China (in Chinese). Hefei: University of Science and Technology of China Press, 2004. 571–646
16 Isozaki Y, Kawahata H, Minoshima K. The Capitanian (Permian) Kamura cooling event: The beginning of the Paleozoic-Mesozoic transition. Palaeoworld, 2007, 16: 16–30
17 Isozaki Y, Kawahata H, Ota A. A unique carbon isotope record across the Guadalupian-Lopingian (Middle-Upper Permian) boundary in mid-oceanic paleo-atoll carbonates: The high-productivity "Kamura event" and its collapse in Panthalassa. Glob Planet Change, 2007, 55: 21–38
18 Erwin D H. Understanding Biotic Recoveries: Extinction, Survival, and Preservation during the End-Permian Mass Extinction. In: Jablonski D, Erwin D H, Lipps J H, eds. Evolutionary Paleobiology. Chicago and London: The University of Chicago Press, 1996. 398–418
19 Yang Z Y, Wu S B, Yin H F. Geological Events of Permo-Triassic Transitional Period in South China (in Chinese). Beijing: Geological Publishing House, 1991

20 Jin Y G, Shen S Z, Henderson C M, et al. The Global Stratotype Section and Point (GSSP) for the boundary between the Capitanian and Wuchiapingian Stage (Permian). Episodes, 2006, 29: 253–262
21 Wignall P B, Sun Y, Bond D P G, et al. Volcanism, mass extinction, and carbon isotope fluctuations in the Middle Permian of China. Science, 2009, 324: 1179–1182
22 Wignall P B, Védrine S, Bond D P G, et al. Facies analysis and sea-level change at the Guadalupian-Lopingian Global Stratotype (Laibin, South China), and its bearing on the end-Guadalupian mass extinction. J Geol Soc London, 2009, 166: 655–666
23 Yang Z Y, Shen W Z, Zheng L D. Elements and isotopic geochemistry of Guadalupian-Lopingian boundary profile at the Penglaitan Section of Laibin, Guangxi Province, and its geological implications (in Chinese). Acta Geol Sin, 2009, 83: 1–15
24 Bond D P G, Wignall P B, Wang W, et al. The mid-Capitanian (Middle Permian) mass extinction and carbon isotope record of South China. Palaeogeogr Palaeoclimat Palaeoecol, 2010, 292: 282–294
25 Courtillot V, Jaupart C, Manighetti I, et al. On causal links between flood basalts and continental breakup. Earth and Planet Sci Lett, 1999, 166: 177–195
26 Hallam A, Wignall P B. Mass extinctions and sea-level changes. Earth-Sci Rev, 1999, 48: 217–250
27 Lai X, Wang W, Wignall P B, et al. Palaeoenvironmental change during the end-Guadalupian (Permian) mass extinction in Sichuan, China. Palaeogeogr Palaeoclimat Palaeoecol, 2008, 269: 78–93
28 Isozaki Y, Yao J, Matsuda T, et al. Stratigraphy of the Middle-Upper Permian and Lowermost Triassic at Chaotian, Sichuan, China. Proc Japan Acad, 2004, 80(B): 10–16
29 He B, Xu Y, Huang X, et al. Age and duration of the Emeishan flood volcanism, SW China: Geochemistry and SHRIMP ziron U-Pb dating of silicic ignimbrites, post-volcanic Xuanwei Formation and clay tuff at the Chaotian section. Earth Planet Sci Lett, 2007, 255: 306–323
30 He B, Xu Y, Zhong Y, et al. The Guadalupian-Loping boundary mudstones at Chaotian (SW China) are clastic rocks rather than acidic tuffs: Implication for a temporal coincidence between the end-Guadalupian mass extinction and the Emeishan volcanism. Lithos, 2010, 119: 10–19
31 Feng Z Z, Yang Y Q, Jin Z K, et al. Lithofacies Paleography of Permian of South China (in Chinese). Beijing: Petroleum University Press, 1997. 60–62
32 Jin Y G, Shang Q H, Wang X D, et al. Chronostratigraphic subdivision and correlation of the Permian in China. Acta Geol Sin, 1999, 73: 127–138
33 Xu Y G, Chung S L, Jahn B M, et al. Petrologic and geochemical constrains on the petrogenesis of Permian-Triassic Emeishan flood basalts in southwestern China. Lithos, 2001, 58: 145–168
34 Chung S L, Jahn B M, Wu G, et al. The Emeishan flood basalt in SW China: A mantle plume initiation model and its connection with continental breakup and amss extinction at the Permian-Triassic boundary. In: Flower M F J, Chung S L, Lo C H, et al, eds. Mantle Dynamics and Plate Interactions in East Asia. Geodynamics Series, Vol 27. Washington DC: American Geophysical Union, 1998. 47–58
35 Jin Y, Shang J. The Permian of China and its interregional correlation. In: Yin H, Dickins J M, Shi G R, et al, eds. Permian-Triassic Evolution of Tethys and Western Circum-Pacific. Developments in Palaeotology and Stratigraphy, Vol 18. Amsterdam: Elsevier, 2000. 71–98
36 Song X Y, Hou Z Q, Wang Y L, et al. The mantle plume features of Emeishan Basalts (in Chinese). J Mineral Petrol, 2002, 22: 27–32
37 Ali J R, Fitton J G, Herzberg C. Emeishan large igneous province (SW China) and the mantle-plume up-doming hypothesis. J Geol Soc London, 2010, 167: 953–959
38 Campbell I H, Griffiths R W. Implications of mantle plume structure for the evolution of flood basalts. Earth Planet Sci Lett, 1990, 99: 79–93
39 Ukstins Peate I, Bryan S E. Re-evaluating plume-induced uplift in the Emeishan large igneous province. Nat Geosci, 2008, 1: 625–629
40 He B, Xu Y G, Chung S L, et al. Sedimentary evidence for a rapid crustal doming before the eruption of the Emeishan flood basalts. Earth Planet Sci Lett, 2003, 213: 389–403
41 He B, Xu Y G, Wang Y M, et al. Sedimentation and lithofacies paleogeography in southwestern China before and after the Emeishan flood volcanism: New insights into surface response to mantle plume activity. J Geol, 2006, 114: 117–132
42 Ali J R, Thompson G M, Song X Y, et al. Emeishan Basalts (SW China) and the 'end-Guadalupian' crisis: Magnetobiostratigraphic constraints. J Geol Soc London, 2002, 159: 21–29
43 Liu C Y, Zhu R. Geodynamic significances of the Emeishan Basalts. Earth Sci Front, 2009, 16: 52–69
44 Sun Y, Lai X, Wignall P B, et al. Dating the onset and nature of the Middle Permian Emeishan large igneous province eruptions in SW China using conodont biostratigraphy and its bearing on mantle plume uplift models. Lithos, 2010, 119: 20–33
45 Huang K, Opdyke H D. Magnetostratigraphic investigations of an Emeishan basalt section in western Guizhou Province, China. Earth Planet Sci Lett, 1998, 163: 1–14
46 Wang W, Cao C Q, Wang Y. The carbon isotope excursion on GSSP candidate section of Loping-Guadalupian boundary. Earth Planet Sci Lett, 2004, 220: 57–67
47 Fenton K C, Holmden C. Sea-level forcing of carbon isotope excursions in epeiric seas: Implications for chemostratigraphy. Canadian J Earth Sci, 2007, 44: 807–818
48 Saltzman M R, Groessens E, Zhuravlev A V. Carbon cycle models based on extreme changes in δ^{13}C: An example from the lower Mississippian. Palaeogeogr Palaeoclimat Palaeoecol, 2004, 213: 331–358
49 Mei S L, Jin Y G, Wardlaw B R. Conodont succession of the Guadalupian-Lopingian boundary strata in Laibin of Guangxi, China and West Texas, USA. Palaeoworld, 1998, 9: 53–76
50 McLean D M. Mantle degassing unification of the Trans-K-T geobiological record. Evolution Biol, 1985, 19: 287–313
51 Self S, Widdowson M, Thordarson T, et al. Volatile fluxes during flood basalt eruptions and potential effects on the global environment: A Deccan perspective. Earth Planet Sci Lett, 2006, 248: 518–532
52 Borowski W S, Paull C K, Ussler W. Carbon cycling within the upper methanogenic zone of continental rise sediments: An example from the methane-rich sediments overlying the Blake Ridge gas hydrate deposit. Mar Chem, 1997, 57: 299–311
53 Boschker H T S, Nold S C, Wellsbury P, et al. Direct linking of microbial populations to specific biogeochemical processes by ^{13}C-labelling of bio-markers. Nature, 1998, 392: 801–805
54 Jahnke L L, Summons R E, Hope J M, et al. Carbon isotope fractionation in lipids from methanotrophic bacterial II: The effects of physiology and environmental parameters on the biosynthesis and isotopic signature of biomarkers. Geoch Cosmoch Acta, 1999, 63: 79–93
55 Hesselbo S P, Grocke D R, Jenkyns H C, et al. Massive dissociation of gas hydrate during a Jurassic oceanic anoxic event. Nature, 2000, 406: 392–395
56 Kamo S L, Czamanske G K, Amelin Y, et al. Rapid eruption of Siberian flood-volcanic rocks and evidence for coincidence with the Permian-Triassic boundary and mass extinction at 251 Ma. Earth Planet Sci Lett, 2003, 214: 75–91
57 Rampino M R, Prokoph A, Adler A. Tempo of the end-Permian event: High-resolution cyclostratigraphy at the Permian-Triassic boundary. Geology, 2000, 28: 643–646
58 Shelf S, Thordarson T, Widdowson M. Gas fluxes from flood basalt eruptions. Elements, 2005, 1: 283–287
59 Isozaki Y. Illawarra Reversal: The fingerprint of a superplume that triggered Pangea breakup and the end-Guadalupian (Permian) mass extinction. Gondwana Res, 2009, 15: 421–432
60 Neumann E R, Olsen K H, Baldridge W S, et al. The Oslo rift: A review. Tectonophysics, 1992, 208: 1–18
61 Larson B T, Olaussen S, Sundvoll B, et al. The Pemo-Carboniferous Oslo rift through six stages and 65 million years. Episodes, 2008, 31: 52–58
62 Rabu D, Le Metour J, Bechennec F, et al. Sedimentary aspects of the Eo-Alpine cycle on the northeast edges of the Arabian Platform (Oman Mountains). In: Robertson A H F, Searle M P, Ries A C, eds. The geology and tectonics of the Oman region. Geol Soc London

Spec Publ, 1990, 49: 49–68
63 Le Maitre R W. Volcanic rocks from EDEL No. 1 petroleum exploration well, offshore Carnavon basin, Western Australia. J Geol Soc Australia, 1975, 22: 167–174
64 Veevers J J, Tewali R C. Permian-Carboniferous and Permian-Triassic magmatism in the rift zone bordering the Tethyan margin of southern Pangea. Geology, 1995, 23: 467–470
65 Parrish J T. Geological Evidence of Permian Climate. In: Scholle P A, Peryt T M, Ulmer-Scholle D S, eds. The Permian of North Pangea Volume 1: Paleogeography, Paleoclimates, Stratigraphy. Berlin-Heidelberg: Springer-Verlag, 1995. 53–61
66 Chenet A L, Fluteau F, Courtillot V. Modelling massive sulphate aerosol pollution, following the large 1783 Laki basaltic eruption. Earth Planet Sci Lett, 2005, 236: 721–731
67 Rampino M R, Stothers R B. Flood basalt volcanism during the past 250 million years. Science, 1988, 241: 663–668
68 Courtillot V. Evolutionary Catastrophes: The Science of Mass Extinction. Cambridge: Cambridge University Press, 1999. 1–237
69 Courtillot V. Mass extinctions in the last 300 million years: One impact and seven flood basalts. Israel J Earth Sci, 1994, 43: 255–266
70 Self S, Blake S, Sharma K, et al. Sulfur and chlorine in Late Cretaceous Deccan magmas and eruptive gas release. Science, 2008, 319: 1654–1657
71 Wignall P B. Large igneous provinces and mass extinctions. Earth Sci Rev, 2001, 53: 1–33
72 Jin Y G, Mei S, Wang W, et al. On the Lopingian Series of the Permian System. Palaeoworld, 1998, 9: 1–18
73 Isozaki Y, Aljinović D, Kawahata H. The Guadalupian (Permian) Kamura event in European Tethys. Palaeogeogr Palaeoclimat Palaeoecol, 2011, 308: 12–21